Available online at www.sciencedirect.com

ScienceDirect

Ceramics International 40 (2014) 2741–2745

CERAMICS INTERNATIONAL

www.elsevier.com/locate/ceramint

Variation in ferroelectric polarization direction of epitaxial (001) $SrBi_2Ta_2O_9$ thin film induced by oxygen vacancy

Jong Yeog Son[a,*], Wan Joo Maeng[b], Woo-Hee Kim[c,*]

[a]*Department of Applied Physics, College of Applied Science, Kyung Hee University, 1732 Deogyeong-daero, Giheung-Gu, Yongin-City 446-701, Republic of Korea*
[b]*Department of Materials Science and Engineering, University of Wisconsin–Madison, Madison, WI 53706, USA*
[c]*Process Development Team, System LSI Division, Samsung Electronics, San #24 Nongseo-Dong, Giheung-Gu, Yongin-City 446-711, Republic of Korea*

Received 1 September 2013; received in revised form 3 September 2013; accepted 13 October 2013
Available online 22 October 2013

Abstract

We report the enhancement of *c*-axis ferroelectric properties in an epitaxial (001) $SrBi_2Ta_2O_9$ (SBT) thin film originating from the oxygen vacancy. We controlled the oxygen vacancy in the SBT thin film by using the electrical stress process triggering the polarization fatigue. As a result of the fatigue test for the Pt/SBT/Nb:STO capacitor, we observed the gradual increase in the ferroelectric polarization up to 10^{12} fatigue cycles and then subsequently rapid decrease over 10^{12} cycles. Based on piezoresponse force microscopy (PFM) measurements, we demonstrated the increase in the polarization and PFM signal resulting from the creation of oxygen vacancy.

Keywords: C. Fatigue; C. Ferroelectric properties; Epitaxial SBT film; PFM

1. Introduction

Spontaneous polarizations in ferroelectric materials make it possible to fabricate nonvolatile random access memories by adjusting the upward and downward directions of a ferroelectric polarization direction [1–5].The spontaneous polarizations in typical ferroelectric materials, except for improper ferroelectric materials such as $SmFeO_3$, originate from crystal structures having a polar axis [6–10]. Most of the inorganic ferroelectric materials, including $PbTiO_3$ and $BiFeO_3$, are perovskite structures consisting of distorted octahedrons below the Curie temperatures [2,7]. For example, $PbTiO_3$ shows a tetragonal structure (P4mm) with a polar axis along the *c*-axis [11]. In contrast to $PbTiO_3$, $SrBi_2Ta_2O_9$ (SBT), a so-called bi-layered Aurivillius compound, is a structure consisting of Bi_2O_2 layers and double perovskite-type TaO_6 octahedral units. The SBT system has a polar axis along the *a*- or *b*-axes, not the *c* axis, although it is a tetragonal structure (A21am) [12]. This is because its mirror inversion symmetry plane is perpendicular to the *c* axis between double perovskite layers. Accordingly, many researches have been focused on improvement of ferroelectric polarizations in SBT thin films by *a*- or *b*-oriented thin film growths because a spontaneous polarization of SBT is perpendicular to the *c*-axis [13–16]. On the contrary, the enhancement of *c*-axis polarization by breaking mirror symmetry has rarely been studied.

Meanwhile, the oxygen vacancy in octahedrons occurs due to a fatigue phenomenon that markedly reduces ferroelectric polarizations by the repetition of ferroelectric polarization switching [17]. In contrast to the fatigue phenomena in ferroelectric thin films, the oxygen vacancy in a paraelectric $SrTiO_3$ (STO) thin film enables it to exhibit room-temperature ferroelectricity [18]. Nevertheless, the effect of oxygen vacancy in a TaO_6 octahedral layer on ferroelectric polarization has not been reported yet. From the mirror symmetry of the *c*-axis, the oxygen vacancy in a double heterostructure layer would affect the ferroelectric polarization due to symmetry breaking. In this study, therefore, we investigated the effect of the oxygen vacancy on the enhanced ferroelectric properties of an epitaxially *c*-oriented SBT thin film. We systematically controlled the degree of the oxygen vacancy by measuring the current as a function of switching cycles. We comparatively studied the fatigue behavior, a ferroelectric hysteresis loop of a SBT capacitor, and the piezoelectric force microscopy for nanoscale local areas depending on the number of switching cycles.

*Corresponding authors. Tel.: +82 31 209 8284; fax: +82 31 201 3770.
E-mail addresses: jyson@khu.ac.kr (J. Yeog Son), hanpos7@gmail.com (W.-H. Kim).

0272-8842/$ - see front matter © 2013 Elsevier Ltd and Techna Group S.r.l. All rights reserved.
http://dx.doi.org/10.1016/j.ceramint.2013.10.046

2. Experimental details

We prepared an epitaxial SBT thin film with a thickness of ~50 nm on an Nb-doped STO (Nb:STO) substrate using pulsed laser deposition (PLD). To produce an atomically flat surface on the Nb:STO substrates (Nb doping level ~1 wt% and resistivity ~0.001 Ω cm), the surfaces of the Nb:STO substrates were etched in a dilute HF solution and then subsequently annealed for 1 h at 1000 °C [19]. A commercially available 1-in yellowish pellet of SBT was employed as a PLD target. A KrF excimer laser (maximum energy = 150 mJ, pulsed duration = 30 ns, 248 nm) was introduced into a stainless steel chamber at an incident angle of 45° and a repetition rate of 2 Hz. Before the substrate was loaded into a vacuum chamber for the SBT thin film deposition, the substrate was cleaned using an ultrasonic cleaner in acetone, methanol, and deionized water. Once the base pressure of $\sim 5 \times 10^{-7}$ Torr was reached, the substrate temperature was set to 800 °C with an oxygen partial pressure of 400 mTorr. After the deposition, the SBT thin film was cooled down to room temperature in oxygen ambient at 400 Torr.

The structure of the SBT thin film was investigated by X-ray diffraction (XRD, Cu Kα radiation 1.542 Å). The thickness of the SBT thin film was measured by cross-sectional scanning electron microscope (SEM). The tentative composition of the SBT thin film was obtained by energy dispersive X-ray spectrometer. The surface morphology and the ferroelectric nanobits of the STO thin film were observed by atomic force microscopy (AFM) and piezoresponse force microscopy (PFM), respectively.

To fabricate circular-shaped top electrodes with a radius of 100 μm, 200 nm-thick Pt was deposited on the SBT films by RF magnetron sputtering through a dot-patterned shadow mask. Subsequently, all the samples were annealed at 400 °C for 5 min prior to obtaining the ferroelectric hysteresis loops, which were measured using an RT66A (Radiant Technologies, Inc.) test system.

3. Results and discussions

To begin with, we investigated the crystallinity of epitaxially grown SBT thin film on the Nb:STO substrate by XRD characterizations. Fig. 1(a) shows the θ–2θ scan of the SBT thin film, indicating the (00l) oriented growth of the SBT thin film. In addition to that, the in-plain φ scans of the (115) peak for the SBT thin film and the (101) peak of the Nb:STO substrate are shown in Fig. 1(b). Two φ scans exhibiting two peaks have fourfold symmetries and the position for the peaks of two φ scans are the same, indicating that the SBT thin film is epitaxially grown along the (00l) orientation.

We observed the surface morphology of the epitaxial (011) SBT thin film by AFM. Fig. 2(a) shows an AFM image of the epitaxial (001) SBT thin film. There are terraces with an interval of about 80 nm due to the layer-by-layer growth mechanism. The epitaxial (001) SBT thin film had an atomically flat surface with a low surface roughness of about 0.5 nm, as shown in Fig. 2(a). To measure the *c*-axis ferroelectric property of the SBT thin film, we observed a hysteresis loop of the out-of-plane Pt/SBT/Nb:STO capacitor at a measurement frequency of 10 kHz, as shown in Fig. 2(b). The Pt/SBT/Nb:STO capacitor exhibited the low remnant polarization of 3 μC/cm^2 with a coercive electric field of about 68 kV/cm. This value is much smaller than the *a*-axis spontaneous polarized value of SBT thin films in a previous report [20]. It is inferred that the SBT thin film was well oriented along the (001) direction and thus, the low polarization of out-of-plane was observed [16].

We carried out an electrical fatigue test for the Pt/SBT/Nb:STO capacitor as shown in Fig. 3(a). We experimentally formed the fatigue in the epitaxial SBT thin film by applying ac bias (5 V, 1 Mhz). The stable polarization value was observed up to 10^8 cycles, which corresponds to the previous report on fatigue properties in SBT thin films [21]. Previously, X-ray photoemission spectroscopy (XPS) showed that the formation of oxygen vacancy in the Bi_2O_2 layer was more facile than in the TaO_6 octahedra [22]. The oxygen vacancy of the Bi_2O_2 layer of the SBT thin film was not critically affected with respect to polarization value, whereas the double perovskite layers between the Bi_2O_2 layers were critical [21]. Thus, it indicates that the initial oxygen vacancy formation without any dielectric degradation under electrical stress up to 10^8 fatigue cycles would be related to the Bi_2O_2 layer. However, at over 10^9 cycles, the polarization value was gradually increased up to 10^{12} fatigue cycles. Accordingly, it can be speculated that the newly formed oxygen vacancy over 10^9 fatigue cycles would be

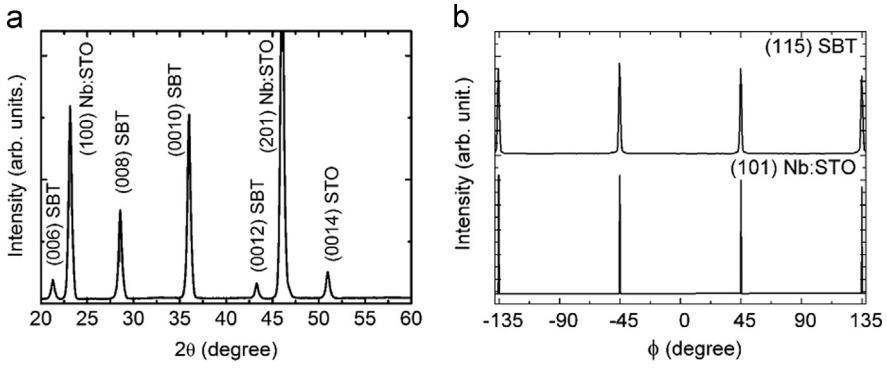

Fig. 1. X-ray diffraction patterns and surface morphology of a ferroelectric hysteresis loop of the epitaxial (001) SBT thin film. (a) θ–2θ scan. (b) φ scans of (115) SBT and (101) Nb:STO.

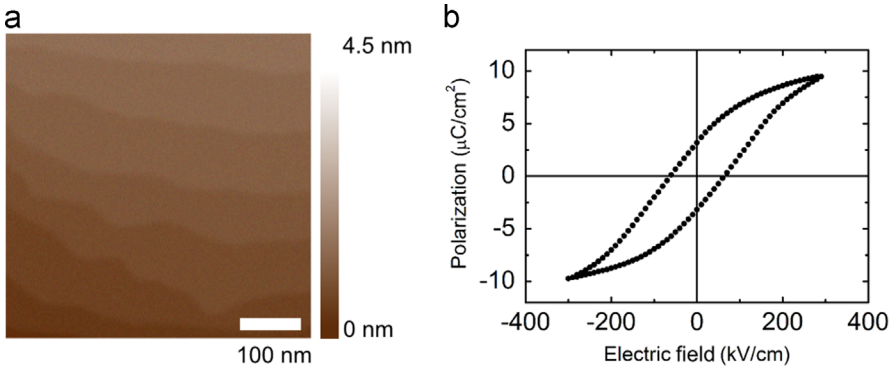

Fig. 2. (a) AFM image of the epitaxial (001) SBT thin film. (b) Ferroelectric hysteresis loop of the epitaxial (001) SBT thin film.

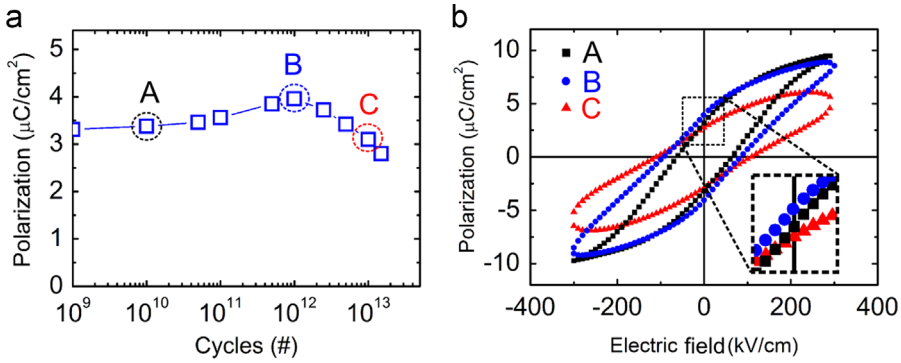

Fig. 3. Typical fatigue behavior of the epitaxial (001) SBT thin film. (a) Polarization as a function of switching cycles for the Pt/SBT/Nb:STO capacitor. (b) Ferroelectric hysteresis loops of the Pt/SBT/Nb:STO capacitor corresponding to points *A*, *B*, and *C* in Fig. 2(a).

generated in the TaO_6 octahedra, which are mainly responsible for the enhancement of ferroelectric polarization. The maximum remnant polarization is approximately 4 μC/cm^2 at 10^{12} fatigue cycles, which is even 30% higher than that of the sample without electrical stress. After reaching the maximum polarization, it rapidly decreased beyond 10^{12} fatigue cycles. This phenomenon can be explained by the conventional fatigue process. From the fatigue under the long-time electrical stress, the electromigration of oxygen vacancy to an interface is more likely to induce an interfacial layer and decrease polarization [17,23]. Fig. 3(b) shows the ferroelectric hysteresis loops of the Pt/SBT/Nb:STO capacitor corresponding to points *A*, *B*, and *C* indicated in Fig. 3(a). No imprint effect was observed among these three samples despite the fatigue process. The highest polarization under 300 kV/cm and the lowest coercive field were observed in the point *A* ($\sim 10^{10}$ cycles) sample. For the case of point *B* ($\sim 10^{12}$ cycles), the Pt/SBT/Nb:STO capacitor had a polarization value of about 9 μC/cm^2 under 300 kV/cm, which is slightly lower than that of point *A*. However, point *C* ($\sim 10^{13}$ cycles) shows almost half the polarization value at 300 kV/cm, compared to points *A* and *B*. The inset of Fig. 3(b) shows the magnified hysteresis graph exhibiting the remnant polarization. The highest remnant polarization was observed at point *B*, while the lowest value was observed at point *C*.

We further investigated ferroelectric characteristics related to the oxygen vacancy in the epitaxial (001) SBT thin film at the nanoscale by *c*-axis PFM experiments in samples A and B. The PFM image of the switched ferroelectric domain revealed a positive surface potential (+1 V), indicating that the ferroelectric polarization was oriented along the field direction in Fig. 4(a) and (c). Then, we subsequently flipped this domain with a bias voltage of −1 V. According to the PFM image in Fig. 4(b) and (d), the ferroelectric domain was perfectly flipped. In other words, Fig. 4(a) and (b) shows PFM images of upward and downward polarization bits for point *A*, and Fig. 4(c) and (d) also exhibits PFM images of upward and downward polarization bits for point *B*. This indicates the well-aligned polarized properties along the *c*-axis for both the samples. However, the brightness differences between the two samples are distinctly observable. The contrast difference between the ferroelectric domain and surrounding area in Fig. 4(c) and (d) is more distinguishable than that in Fig. 4 (a) and (b). This implies that the upward and downward polarization bits of point *B* have larger PFM signals than those for point *A*.

Fig. 5 depicts schematic drawings illustrating the variation in the polarization direction of SBT induced by the generation of oxygen vacancy. Fig. 5(a) illustrates the layered perovskite structure of SBT. Spontaneous polarization is built up perpendicular to the *c*-axis of SBT because the spontaneous polarization direction of the SBT thin film is along the *a*- or *b*-axis. In contrast, the *c*-axis polarization is not observed due to mirror inversion symmetry between the double perovskite layers. As shown in Fig. 5(b), one oxygen vacancy from the

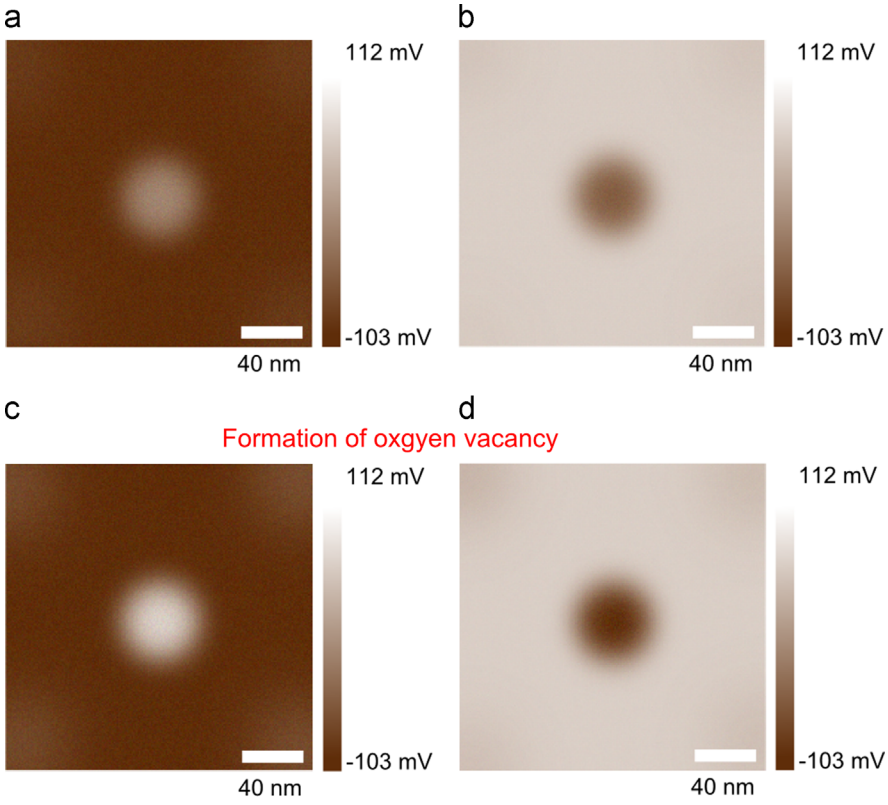

Fig. 4. PFM images of ferroelectric polarization bits for points *A* and *B* indicated in Fig. 3: (a) Upward polarization and (b) downward polarization for point *A*. (c) Upward polarization and (d) downward polarization for point *B*.

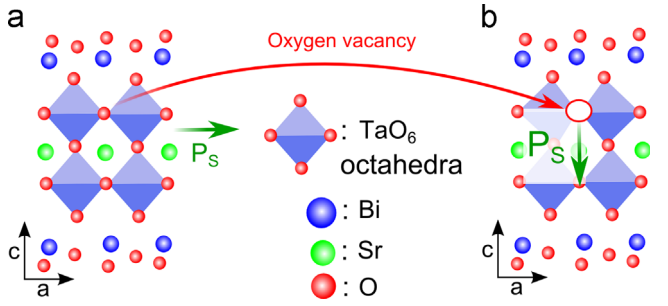

Fig. 5. Schematic drawings illustrating the variation in the polarization directions of SBT induced by oxygen vacancy. (a) The layered perovskite structure of SBT. Polarization direction is along the *a*- or *b*-axis in SBT. (b) Oxygen vacancy in SBT. The oxygen vacancy induces the variation of polarization direction.

fatigue over 10^{12} electric stress cycles induces the distortion of the two TaO_6 octahedrons and the breaking of mirror inversion symmetry. This distortion can induce spontaneous polarization along the *c*-axis [12].

4. Conclusion

In summary, we experimentally created the electrical fatigue in the epitaxial (001) SBT thin film by applying an AC bias. Prior to employing the fatigue, The Pt/SBT/Nb:STO capacitor exhibited a low remnent polarization of 3 μC/cm^2 with a coercive electric field of about 68 kV/cm. However, the electrical fatigue test revealed that the polarization gradually increased at 4 μC/cm^2 up to 10^{12} switching cycles and then decreased rapidly. To make an oxygen vacancy in the TaO_6 octahedral layer, over 10^8 cycles of electronic stress were necessary because the oxygen vacancy of Bi_2O_2 layer, which is not affected in c-axis polarization, is more unstable. Based upon the PFM studies, enhanced polarization and PFM signal were observed for the point B sample with 10^{12} fatigue cycles. Finally, we proposed the schematic model illustrating the variation in the polarization direction in the SBT thin film from *a*- or *b*-axis to *c*-axis introducing the oxygen vacancy.

Acknowledgments

This work was supported by the National Research Foundation of Korea Grant funded by the Korean Government (No. 2012R1A2A2A01046451).

References

[1] J.F. Scott, C.A.P.D. Araujo, Ferroelectric memories, Science 246 (1989) 1400–1405.
[2] J. Wang, J.B. Neaton, H. Zheng, V. Nagarajan, S.B. Ogale, B. Liu, D. Viehland, V. Vaithyanathan, D.G. Schlom, U.V. Waghmare, N.A. Spaldin, K.M. Rabe, M. Wuttig, R. Ramesh, Epitaxial $BiFeO_3$ multiferroic thin film heterostructures, Science 299 (2003) 1719–1722.
[3] J.Y. Son, S. Ryu, Y.-C. Park, Y.-T. Lim, Y.-S. Shin, Y.-H. Shin, H. M. Jang, A nonvolatile memory device made of a ferroelectric polymer gate nanodot and a single-walled carbon nanotube, ACS Nano 4 (2010) 7315–7320.

[4] J.F. Scott, Applications of modern ferroelectrics, Science 315 (2007) 954–959.
[5] I. Jung, J.Y. Son, A nonvolatile memory device made of a graphene nanoribbon and a multiferroic $BiFeO_3$ gate dielectric layer, Carbon 50 (2012) 3854–3858.
[6] J.-H. Lee, Y.K. Jeong, J.H. Park, M.-A. Oak, H.M. Jang, J.Y. Son, J. F. Scott, Spin-canting-induced improper ferroelectricity and spontaneous magnetization reversal in $SmFeO_3$, Phys. Rev. Lett. 107 (2011) 117201-1–117201-3.
[7] Y. Shimakawa, Y. Kubo, Y. Nakagawa, T. Kamiyama, H. Asano, F. Izumi, Crystal structures and ferroelectric properties of $SrBi_2Ta_2O_9$ and $Sr_{0.8}Bi_{2.2}Ta_2O_9$, Appl. Phys. Lett. 74 (1999) 1904–1906.
[8] Y. Shimakawa, Y. Kubo, Y. Tauchi, H. Asano, T. Kamiyama, F. Izumi, Z. Hiroi, Crystal and electronic structures of $Bi_{4-x}La_xTi_3O_{12}$ ferroelectric materials, Appl. Phys. Lett. 79 (2001) 2791–2793.
[9] K. Sone, H. Naganuma, T. Miyazaki, T. Nakajima, S. Okamura, Crystal structures and electrical properties of epitaxial $BiFeO_3$ thin films with (001), (110), and (111) orientations, Jpn. J. Appl. Phys. 49 (2010) (09MB03–09MB03-6).
[10] L. Cheng, G. Hu, B. Jiang, C. Yang, W. Wu, S. Fan, Enhanced piezoelectric properties of epitaxial w-doped $BiFeO_3$ thin films, Appl. Phys. Express 3 (2010) 101501-1–101501-3.
[11] A.A. Belik, M. Azuma, T. Saito, Y. Shimakawa, M. Takano, Crystallographic features and tetragonal phase stability of $PbVO_3$, a new member of $PbTiO_3$ family, Chem. Mater. 17 (2004) 269–273.
[12] C.H. Hervoches, A. Snedden, R. Riggs, S.H. Kilcoyne, P. Manuel, P. Lightfoot, Structural behavior of the four-layer aurivillius-phase ferroelectrics $SrBi_4Ti_4O_{15}$ and $Bi_5Ti_3FeO_{15}$, J. Solid State Chem. 164 (2002) 280–291.
[13] J.H. Cho, S.H. Bang, J.Y. Son, Q.X. Jia, Control of epitaxial growth for $SrBi_2Ta_2O_9$ thin films, Appl. Phys. Lett. 72 (1998) 665–667.
[14] H.N. Lee, D.N. Zakharov, S. Senz, A. Pignolet, D. Hesse, Epitaxial growth of ferroelectric $SrBi_2Ta_2O_9$ thin films of mixed (100) and (116) orientation on $SrLaGaO_4$(110), Appl. Phys. Lett. 79 (2001) (2961–2693).
[15] H.N. Lee, D. Hesse, N. Zakharov, U. Gosele, Ferroelectric $Bi_{3.25}La_{0.75}Ti_3O_{12}$ films of uniform a-axis orientation on silicon substrates, Science 296 (2002) 2006–2009.
[16] S. Zhang, J. Liu, F. Chen, Z. Tian, C. Yang, Ferroelectric property dependence on the texture of $SrBi_2Ta_2O_9$ thin films, Integr. Ferroelectr. 70 (2005) 99–105.
[17] M. Dawber, J.F. Scott, A model for fatigue in ferroelectric perovskite thin films, Appl. Phys. Lett 76 (2000) 1060–1062.
[18] Y.S. Kim, D.J. Kim, T.H. Kim, T.W. Noh, J.S. Choi, B.H. Park, J. G. Yoon, Observation of room-temperature ferroelectricity in tetragonal strontium titanate thin films on $SrTiO_3$ (001) substrates, Appl. Phys. Lett. 91 (2007) 042908-1–042908-3.
[19] M. Kawasaki, K. Takahashi, T. Maeda, R. Tsuchiya, M. Shinohara, O. Ishiyama, T. Yonezawa, M. Yoshimoto, H. Koinuma, Atomic control of the $SrTiO_3$ crystal surface, Science 266 (1994) 1540–1542.
[20] J.-K. Lee, B. Park, K.-S. Hong, Effect of excess Bi_2O_3 on the ferroelectric properties of $SrBi_2Ta_2O_9$ ceramics, J. Appl. Phys. 88 (2000) 2825–2829.
[21] B.S. Kang, B.H. Park, S.D. Bu, S.H. Kang, T.W. Noh, Different fatigue behaviors of $SrBi_2Ta_2O_9$ and Bi_3TiTaO_9 films: role of perovskite layers, Appl. Phys. Lett. 75 (1999) 2644–2646.
[22] B.H. Park, S.J. Hyun, S.D. Bu, T.W. Noh, J. Lee, H.-D. Kim, T.H. Kim, W. Jo, Differences in nature of defects between $SrBi_2Ta_2O_9$ and $Bi_4Ti_3O_{12}$, Appl. Phys. Lett. 74 (1999) 1907–1909.
[23] R.-A. Eichel, Structural and dynamic properties of oxygen vacancies in perovskite oxides—analysis of defect chemistry by modern multi-frequency and pulsed EPR techniques, Phys. Chem. Chem. Phys. 13 (2011) 368–384.